Figure A-10-3. Tc-99 horizontal vadose zone concentrations (pCi/L) for the highest conductance case (MCL = thick red, MCL/10 = thin black, MCL*10 = thin red).

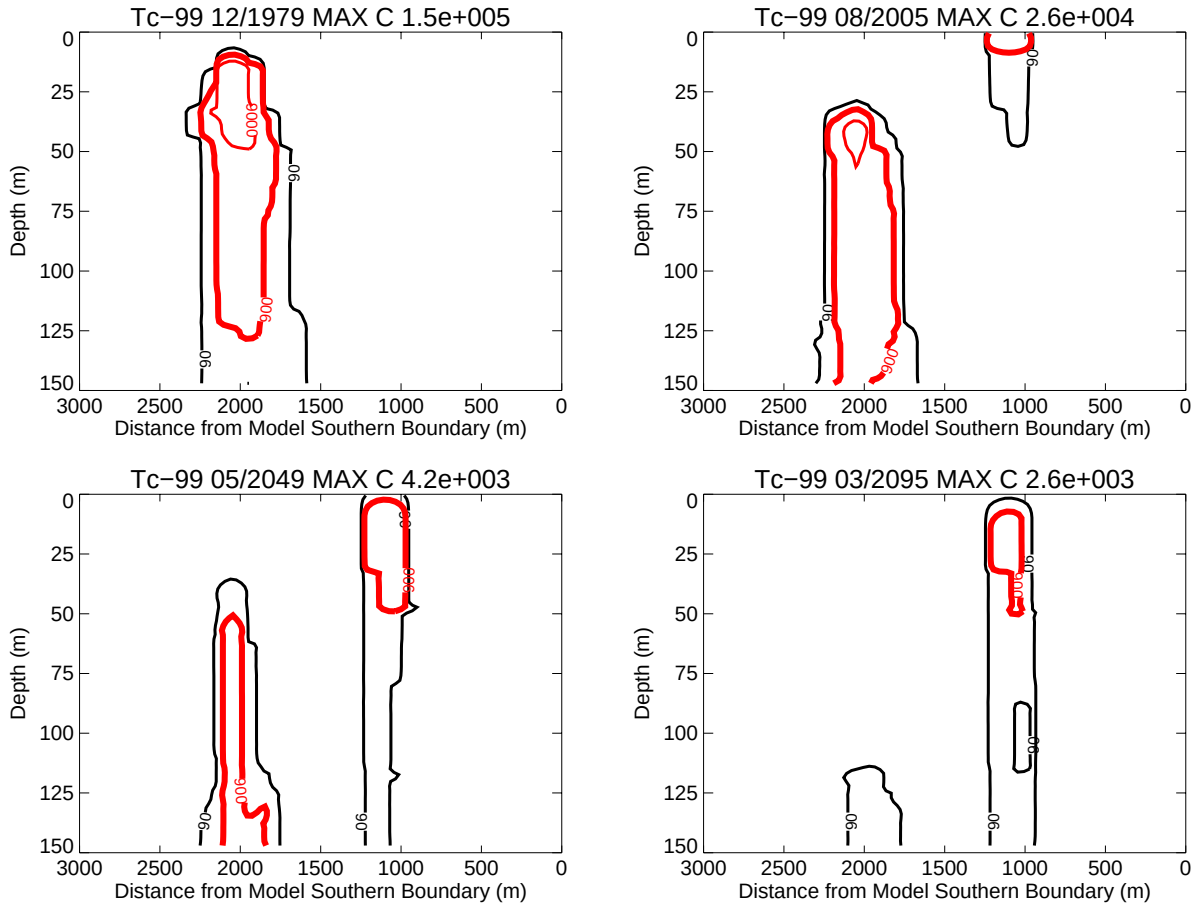

Figure A-10-4. Tc-99 vertical vadose zone concentrations (pCi/L) for the highest conductance case (MCL = thick red, MCL/10 = thin black, MCL*10 = thin red).

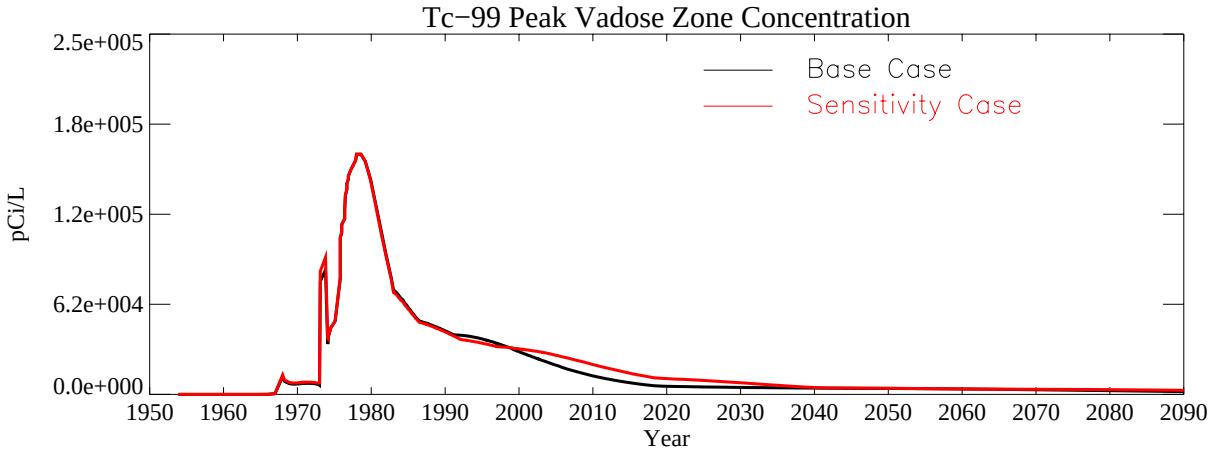

Figure A-10-5. Tc-99 peak vadose zone concentrations (excluding submodel area) (pCi/L) for the highest conductance case.

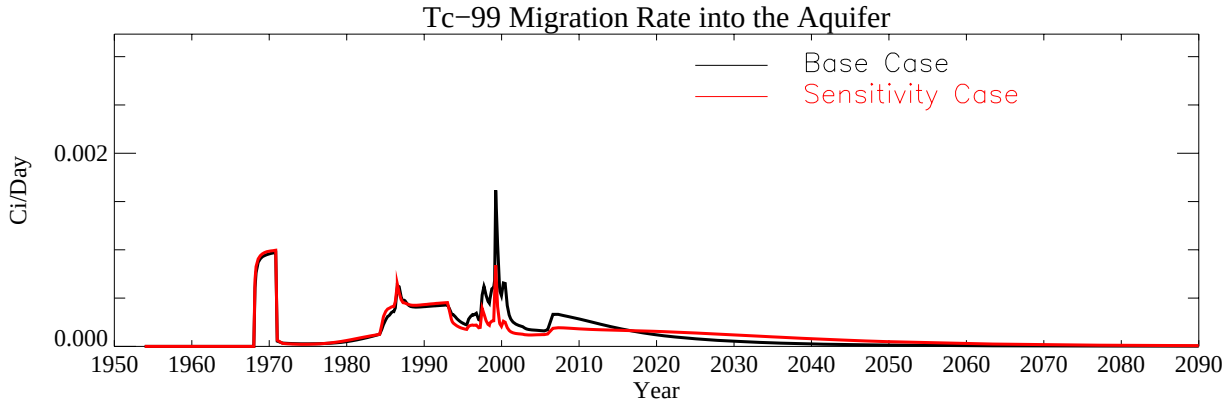

Figure A-10-6. Tc-99 flux into the aquifer (Ci/day) for the highest conductance case.

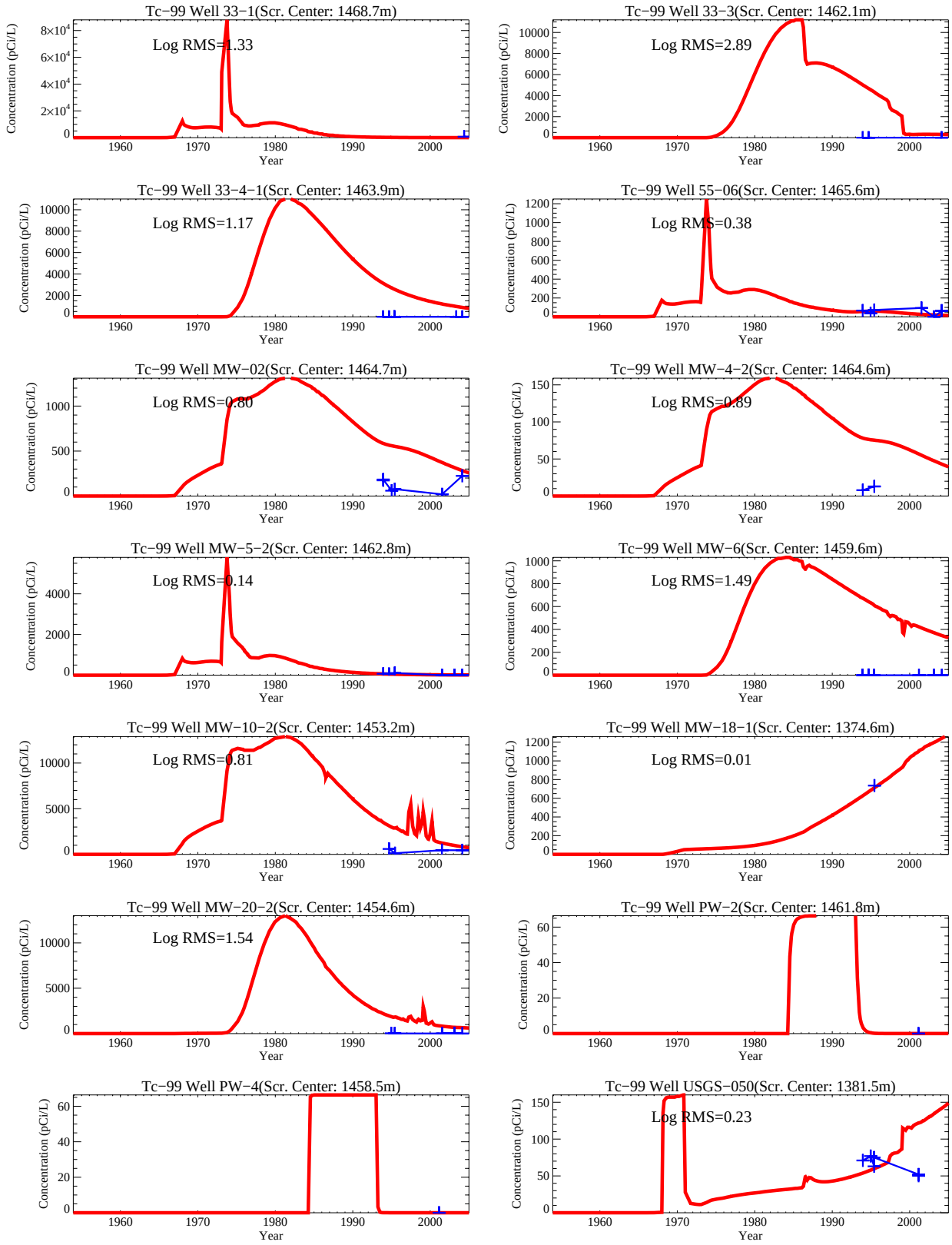

Figure A-10-7. Tc-99 concentration (pCi/L) in perched water wells for the highest conductance case (measured values = blue crosses, red = model at screen center).

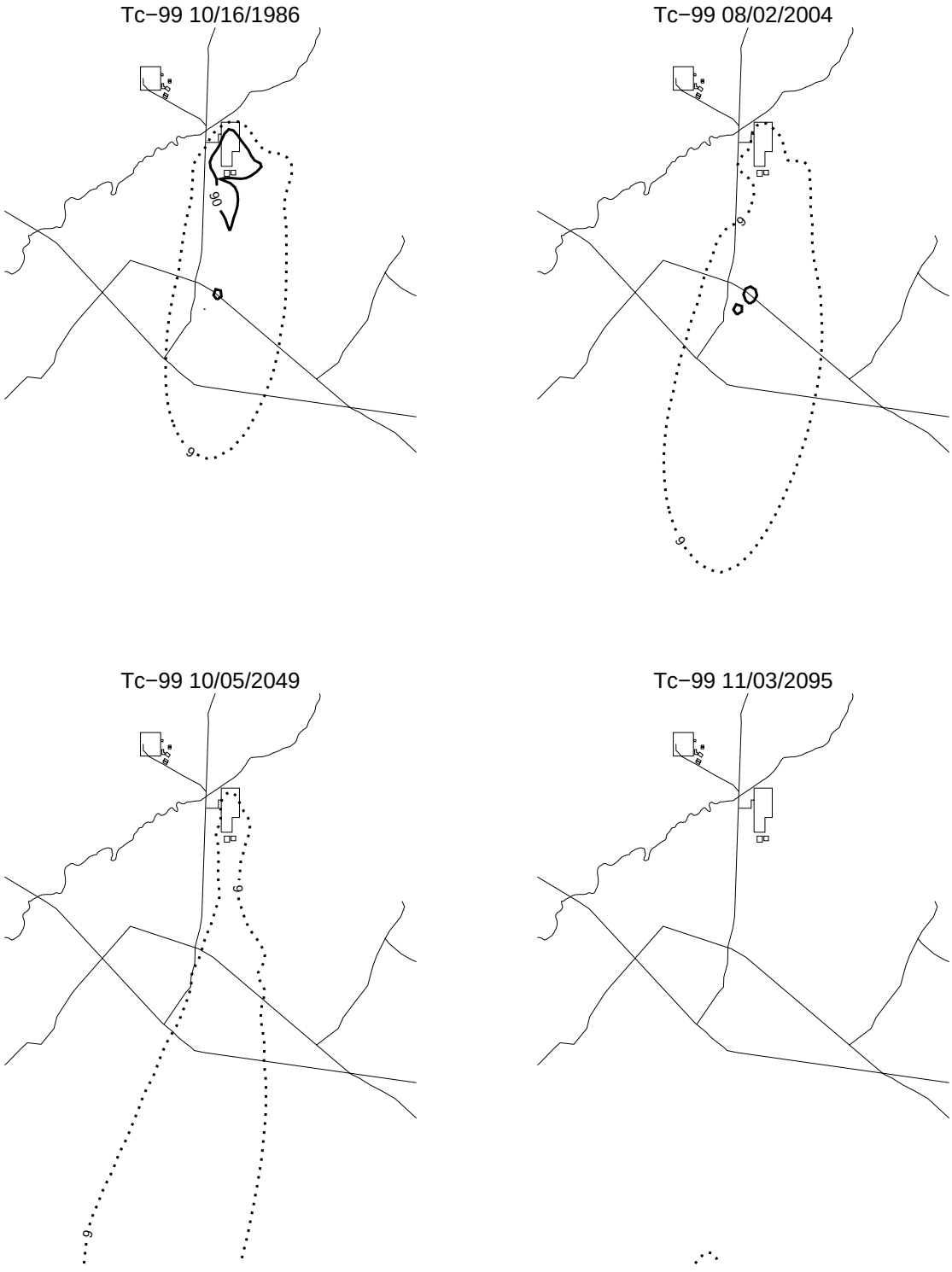

Figure A-10-8. Tc-99 aquifer concentrations (pCi/L) for the highest conductance case (MCL*10 = thin red, MCL = thick red, MCL/10 = thin black, MCL/100 = thin black dashed).

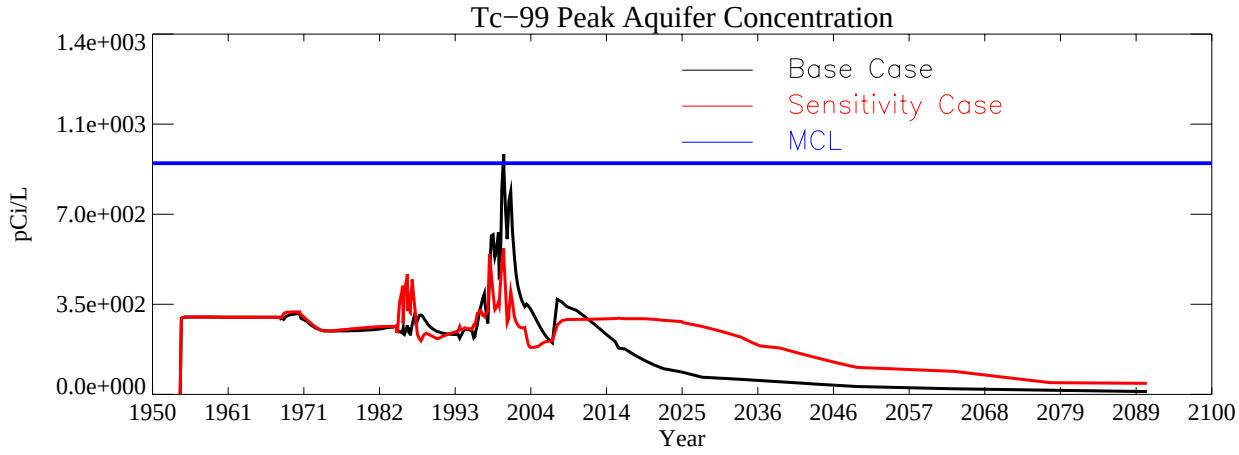

Figure A-10-9. Tc-99 peak aquifer concentrations (pCi/L) for the highest conductance case.

A-10.1.1.2 Lowest Interbed Conductance for Tc-99

The peak simulated concentration in the vadose zone for this case was 1.64e+5 pCi/L in 1972 and coincides with the CPP-31 release date. The simulated peak concentration declined to 2.71e+4 pCi/L in 2005 and to 2.56e+3 pCi/L in 2095. Figures A-10-10 and A-10-11 illustrate the vertical and lateral extent of the simulated vadose zone concentrations. The shallow vadose zone contamination located immediately northwest of the former percolation ponds is due to the CPP-22 OU 3-13 soil site (0.1 Ci), which was placed in the model in 1990.

Figure A-10-12 illustrates the peak vadose zone concentration through time. The Tc-99 activity flux into the aquifer is illustrated in Figure A-10-13 and indicates that the peak rate occurred during the CPP-3 injection well failure period. A second maximum occurred in the year 1999 following the peak flow year for the Big Lost River recorded at Lincoln Boulevard bridge gauge from the tank farm releases. As with the minimum interbed sensitivity simulation, the Big Lost River does not spread as far horizontally and does not increase activity arrival in the aquifer to the same extent as the base case. This was not expected and is because the maximum interbed simulation has a different slope for the 110-ft interbed and does not direct as much river water towards the tank farm. The Tc-99 concentration in key perched water wells is illustrated in Figure A-10-14.

The effect of decreasing the interbed permeability and increasing thickness was similar to that of the minimum thickness and maximum permeability because both sensitivity realizations of the vadose zone lithology decreased the dip of the 140-ft interbed towards the tank farm. The result was that the Big Lost River water did not move as far horizontally towards the tank farm as the base case and the mass flux into the aquifer after the Big Lost River's peak flow year recorded at Lincoln Boulevard bridge gauge in 1999 was less than the base case.

Figure A-10-15 illustrates the horizontal aquifer concentrations, and peak aquifer concentrations through time are given in Figure A-10-16. The maximum interbed sensitivity case decreased the peak aquifer concentrations at the water table from the peak Big Lost River flow year in 1999. During higher flow years the Big Lost River influence was less than the base case. This result is counter intuitive, but occurs because the increased interbed realization's 140 foot interbed did not slope towards the tank farm to the same extent as the base case. The peak aquifer concentration in the year 2095 was 45 pCi/L and was nearly four times the base case.

Figure A-10-10. Tc-99 horizontal vadose zone concentrations (pCi/L) for the lowest conductance case (MCL = thick red, MCL/10 = thin black, MCL*10 = thin red).

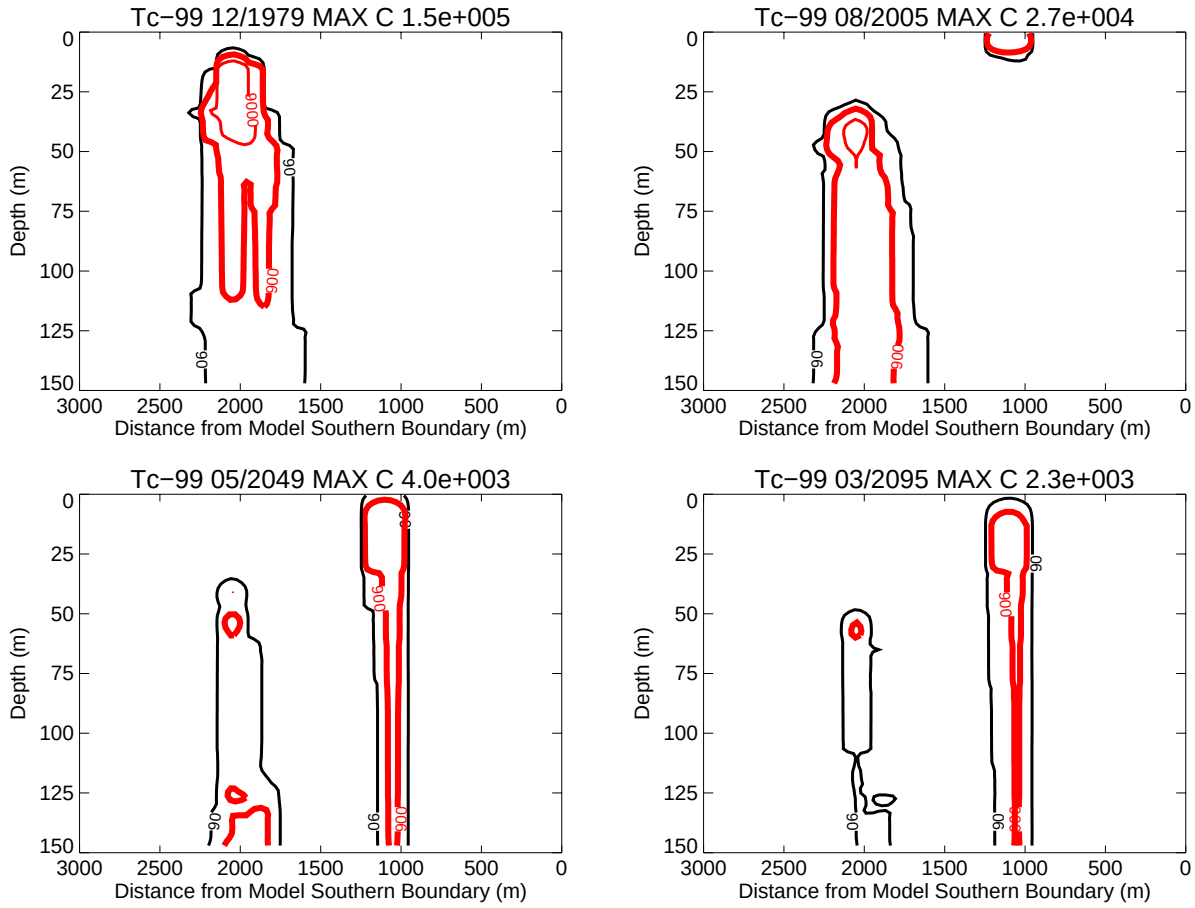

Figure A-10-11. Tc-99 vertical vadose zone concentrations (pCi/L) for the lowest conductance case (MCL = thick red, MCL/10 = thin black, MCL*10 = thin red).

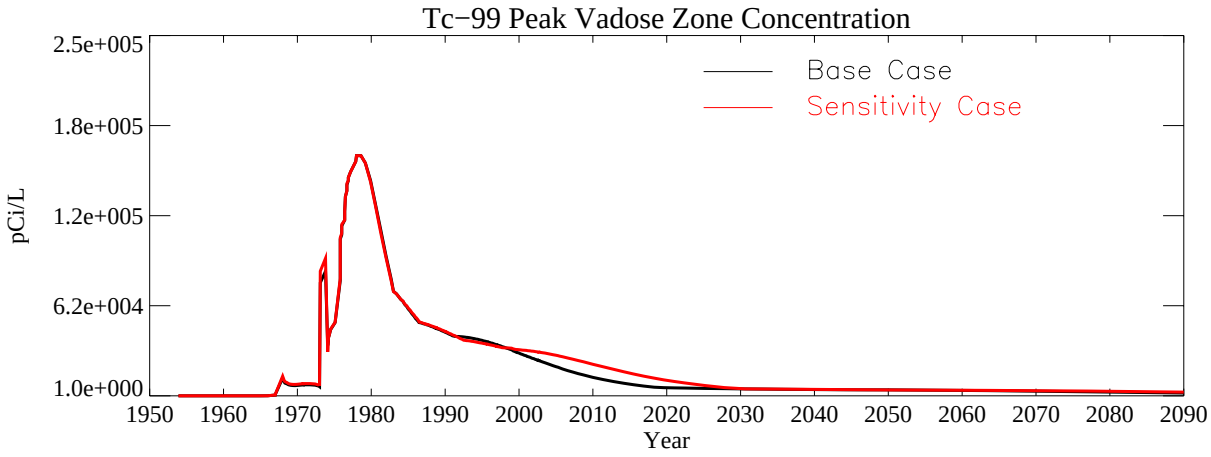

Figure A-10-12. Tc-99 peak vadose zone concentrations (excluding submodel area) (pCi/L) for the lowest conductance case.

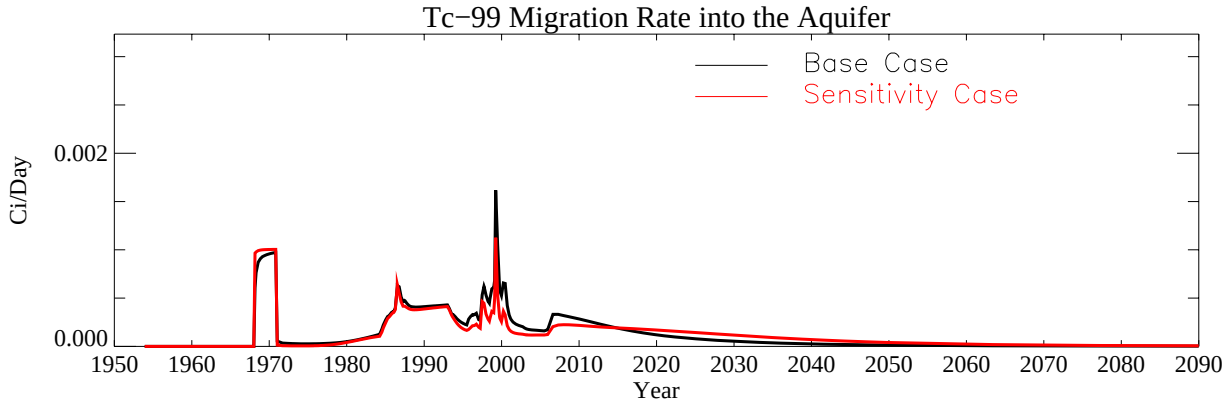

Figure A-10-13. Tc-99 flux into the aquifer (Ci/day) for the lowest conductance case.

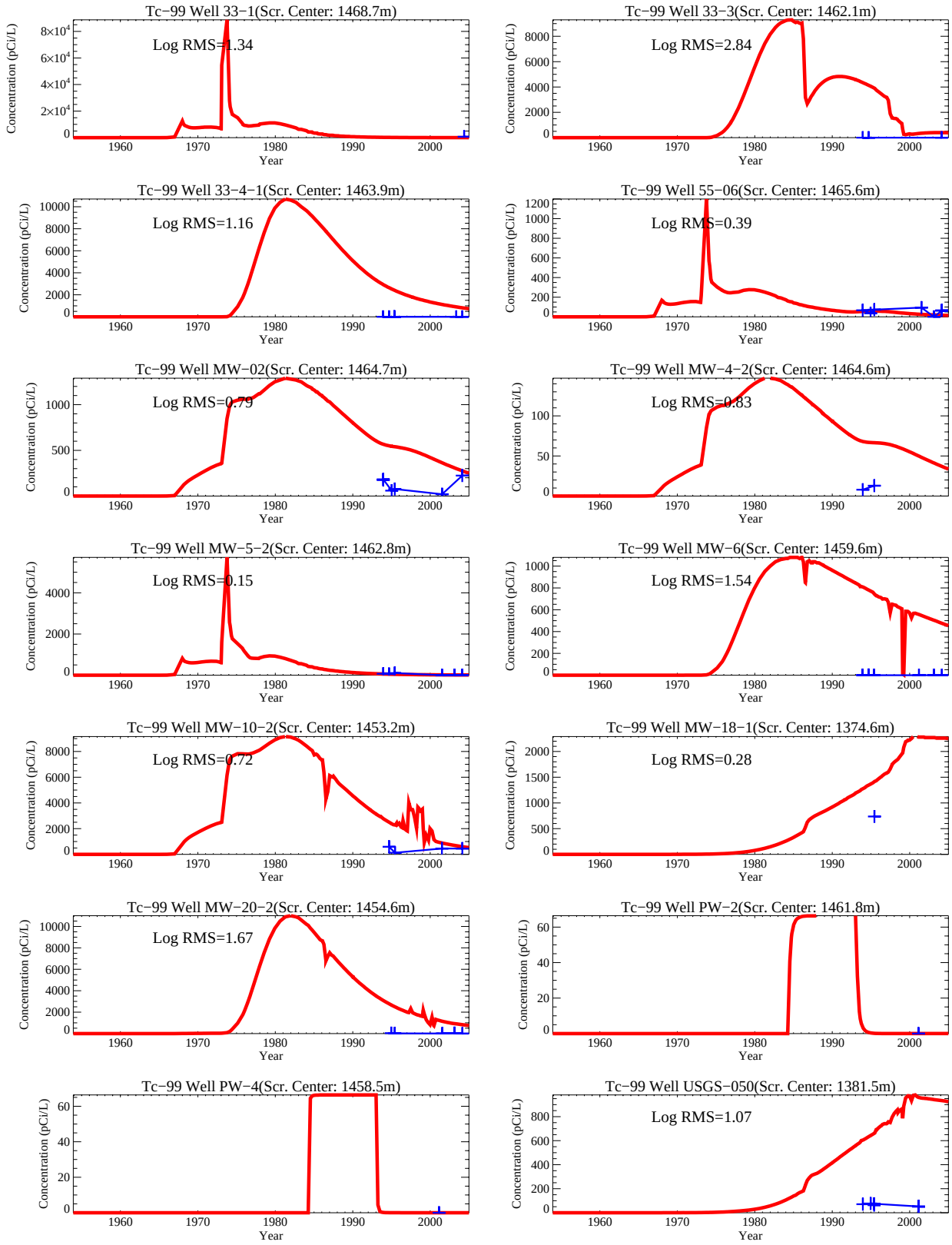

Figure A-10-14. Tc-99 concentrations (pCi/L) for the lowest conductance case (measured values = blue crosses, red = model at screen center).

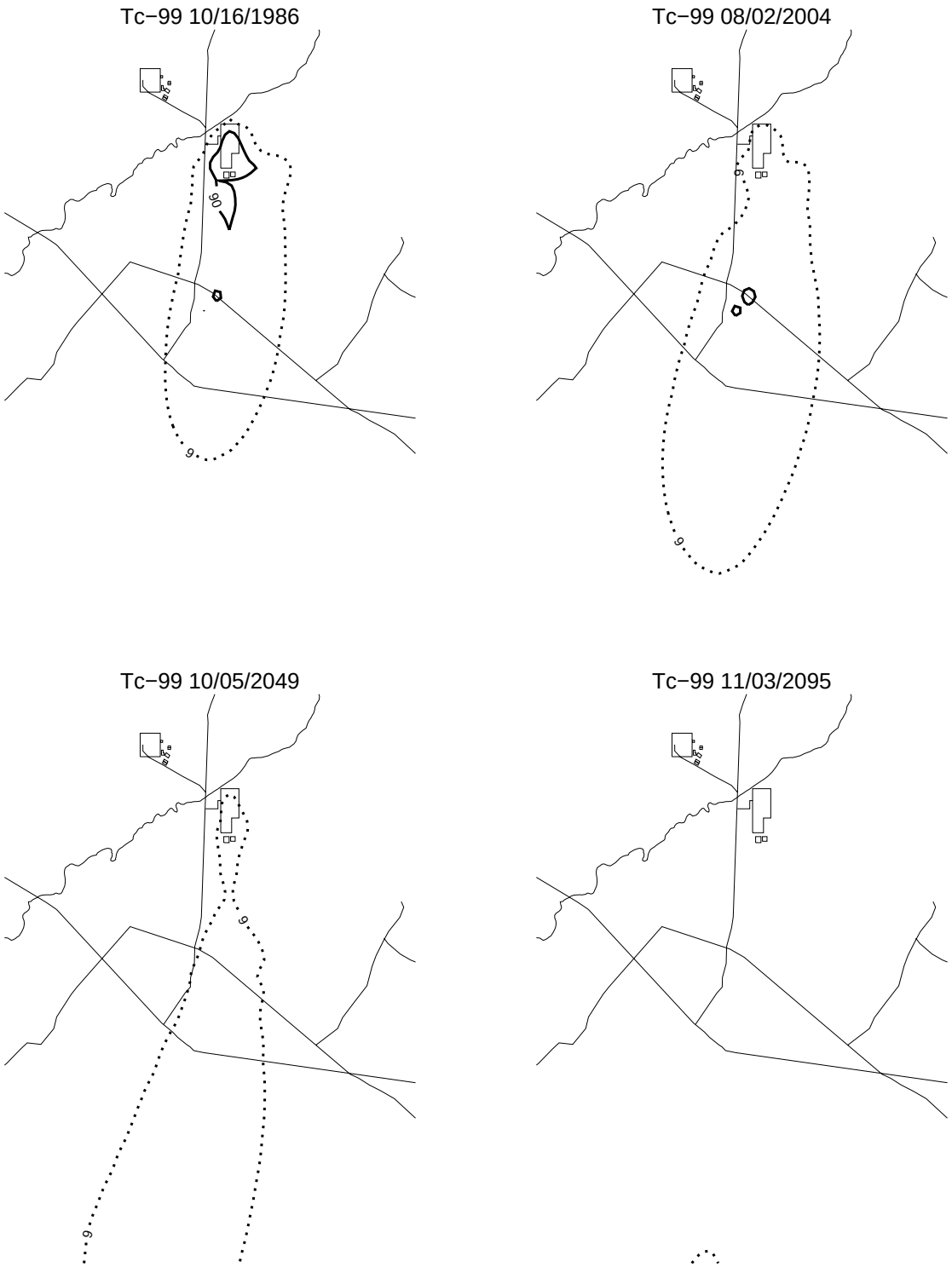

Figure A-10-15. Tc-99 aquifer concentrations (pCi/L) for the lowest conductance case (MCL*10 = thin red, MCL = thick red, MCL/10 = thin black, MCL/100 = thin black dashed).

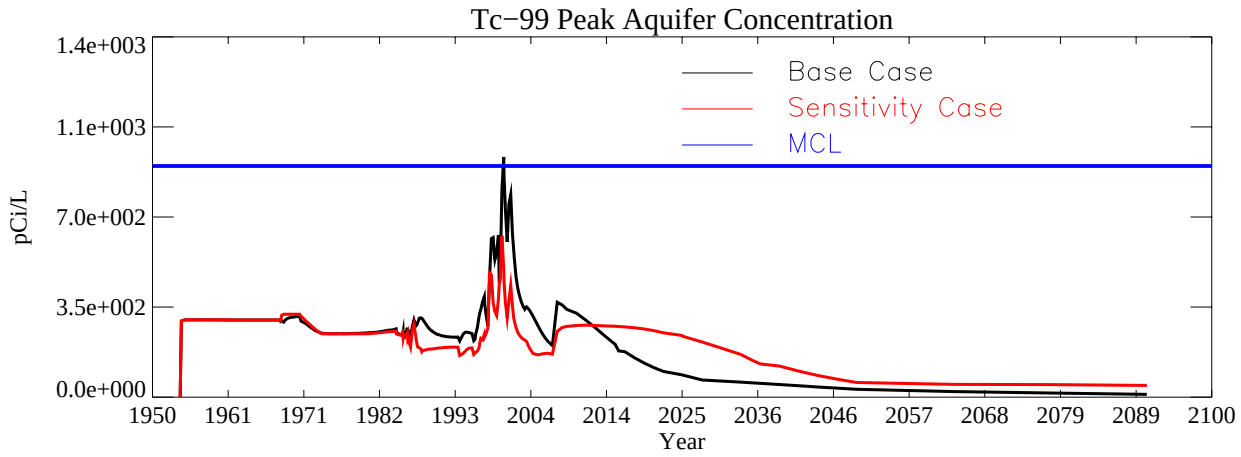

Figure A-10-16. Tc-99 peak aquifer concentrations (pCi/L) for the lowest conductance case.

A-10.1.2 Recharge Rate

Infiltrating water moving down through the contaminated soil mobilizes contaminants and eventually transports them to the aquifer. It is the primary mechanism by which tank farm sources contaminate the Snake River Plain Aquifer. In the base case simulations, the infiltration rate was spatially varying across the INTEC, with an average value, excluding the Big Lost River and former percolation ponds, of 29 cm/year being applied. This value included approximately 11 cm/year of anthropogenic water (i.e., lawn irrigation, steam vents, line leaks, etc.) and 18 cm/year of precipitation infiltration. The base case known recharge sources were applied at the known location (i.e., lawn irrigation areas or sanitary sewer systems [septic tanks] not using the central sewage treatment lagoon). The location of the water supply and fire suppression lines leaks are unknown, and the estimated recharge was uniformly distributed across the entire INTEC facility. The volumetric total of all anthropogenic water sources was approximately 9 M gal/year.

The base case simulated infiltration rate through the tank farm was limited to a precipitation infiltration rate of only 18 cm/year because the net infiltration through the tank farm was calculated through parameter estimation using tank farm soil moisture measurements taken during the spring of 1994 (see Appendix B). The resultant precipitation infiltration rate was determined to be spatially variable across the tank farm and ranged from 2.8 cm/year to 39 cm/year with an average value of 18 cm/year.

The model's sensitivity to the tank farm recharge rate and anthropogenic recharge rate outside the tank farm was investigated by applying a high and low value in place of the 18 cm/year through the tank farm and by using the maximum possible anthropogenic recharge rate outside the tank farm. The recharge sensitivity investigation included three simulations: (1) a low tank farm infiltration rate (3 cm/year) with base case anthropogenic recharge outside the tank farm, (2) a high tank farm infiltration rate (39 cm/year) with base case anthropogenic recharge, and (3) a maximum anthropogenic recharge rate estimated from the water production/ disposal imbalance (maximum of 52 M gal assuming all water is accurately metered and there are no losses to evaporation) with the base case tank farm recharge (18 cm/year).

The maximum anthropogenic recharge scenario represents the worst possible case for water infiltration to the northern perched water and assumes the following: (1) all unaccounted water goes into the ground, (2) the values from the 2004 water balance can be applied to any general time frame, and (3) all water infiltrates in northern INTEC around the high-density infrastructure area.

The maximum anthropogenic recharge rate was estimated from the water imbalance between water production and known final disposal. Recent monitoring of the INTEC water production and final use indicates

that approximately 10 to 11% of the water produced is unaccounted for. The total water usage in 2004 was approximately 495 M gal and 10.5% of this volume suggests an upper maximum of approximately 52 M gal could be discharged to the ground. However, this assumes all water meters are accurate and there are no losses to evaporation. The density of utilities at the INTEC also suggests that the discharge would be focused on northern INTEC in an area of approximately 49 acres surrounding the tank farm.

The maximum anthropogenic water recharge scenario was simulated by using the 2004 water imbalance recharge rate resulting from 52 M gal infiltrating across 49 acres (98 cm/year). This infiltration was in addition to the estimated recharge from infiltration of 18 cm/year (116 cm/year total). The simulated water was placed in the area surrounded by Palm Avenue, Hemlock Street, Ash Avenue, and the western INTEC security fence. The area beneath Building CPP-666 was also included. The area directly below the tank farm area was excluded and used the 18-cm/year precipitation recharge, because most utilities do not run through the tank farm and the high and low tank farm infiltration sensitivity simulations assessed the sensitivity of tank farm contaminant mobility to recharge rate. Sections A-10.1.2.1 and A-10.1.2.2 present the results of the low and high tank farm recharge rate sensitivity, respectively. Section A-10.1.2.3 presents the results of the maximum anthropogenic recharge rate sensitivity.

A-10.1.2.1 Tc-99 with 3-cm/year Tank Farm Recharge Rate

The peak simulated concentration in the vadose zone for this case was 1.01e+6 pCi/L in 1977 and occurs after the CPP-31 release date. The peak simulated concentration declined to 5.47e+4 pCi/L in 2005 and to 8.26e+3 pCi/L in 2095. Figures A-10-17 and A-10-18 present the vertical and lateral extent of the simulated vadose zone concentrations. The shallow vadose zone contamination located immediately northwest of the former percolation ponds is due to the CPP-22 OU 3-13 soil site (0.1 Ci), which was placed in the model in 1990.

Figure A-10-19 shows the peak vadose zone concentration through time and shows that the predicted peak vadose zone concentration remained above the MCL throughout the end of the simulation in 2095. Peak vadose zone concentrations are slightly higher than the base case. The Tc-99 activity flux into the aquifer is illustrated in Figure A-10-20 and shows that the peak Tc-99 flux into the aquifer during peak Big Lost River flow is less than the base case. This is because Tc-99 moves slower through the vadose zone and less Tc-99 resides in the 380-ft interbed during peak river flows. The Tc-99 concentration in key perched water wells is illustrated in Figure A-10-21.

Figure A-10-22 illustrates the horizontal aquifer concentrations, and the peak aquifer concentrations through time are given in Figure A-10-23. Peak aquifer concentrations resulting from the minimum recharge simulation are less than the base case, because the lower infiltration does place the bulk of the tank farm Tc-99 in the 380 ft interbed during peak Big Lost River flow (1999). The majority of the Tc-99 is higher in the vadose zone, where the influence of the river is less. The peak concentration in the year 2095 is 39 pCi/L, which is higher than the base case. This is because the lower infiltration rate results in a slower breakthrough to the aquifer. The base case Tc-99 concentrations have been declining for a longer period of time at the year 2095 than the 3-cm/year infiltration rate case.

Figure A-10-17. Tc-99 horizontal vadose zone concentrations (pCi/L) for the 3-cm/year tank farm recharge rate case (MCL = thick red, MCL/10 = thin black, MCL*10 = thin red).

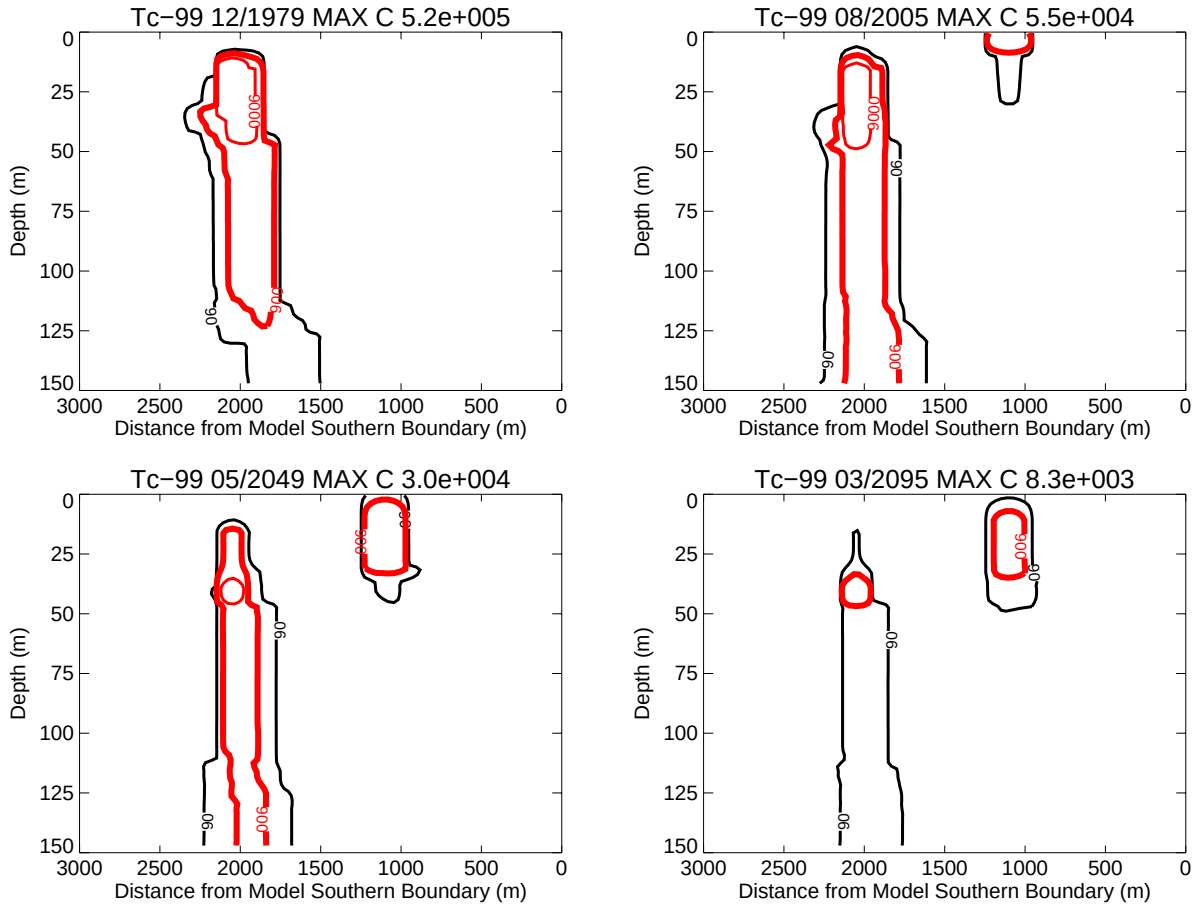

Figure A-10-18. Tc-99 vertical vadose zone concentrations (pCi/L) for the 3-cm/year tank farm recharge rate case (MCL = thick red, MCL/10 = thin black, MCL*10 = thin red).

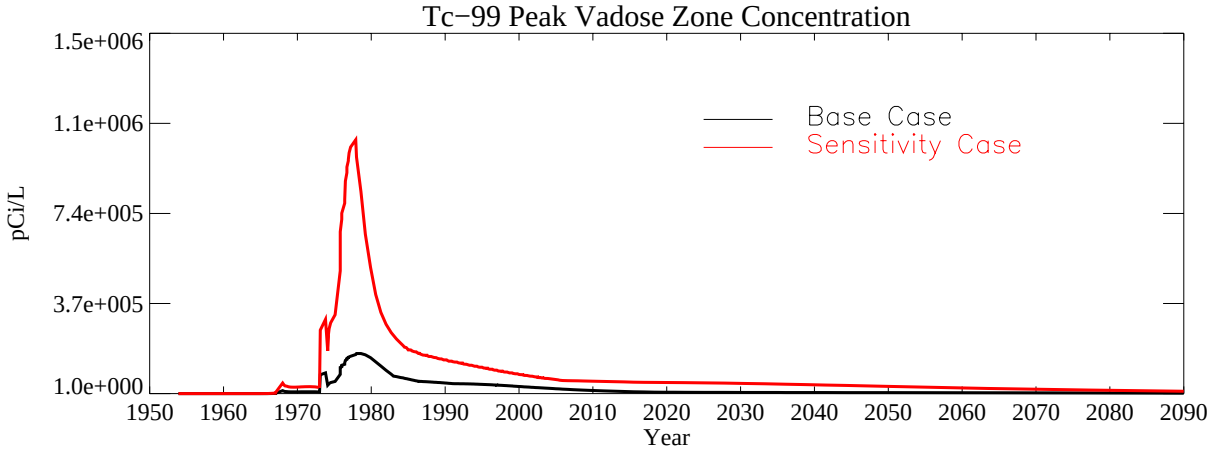

Figure A-10-19. Tc-99 peak vadose zone concentrations (pCi/L) (excluding submodel area) for the 3-cm/year tank farm recharge rate case.

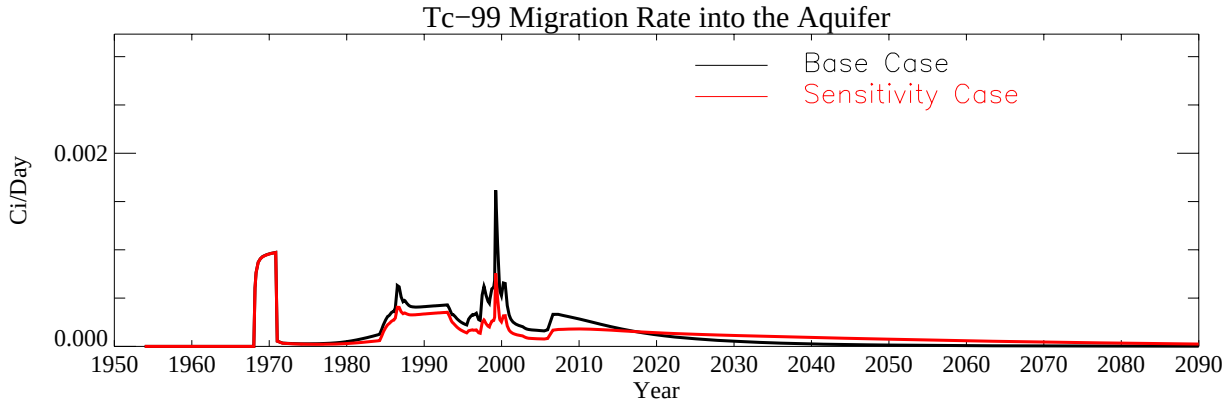

Figure A-10-20. Tc-99 flux into the aquifer (Ci/day) for the 3-cm/year tank farm recharge rate case.

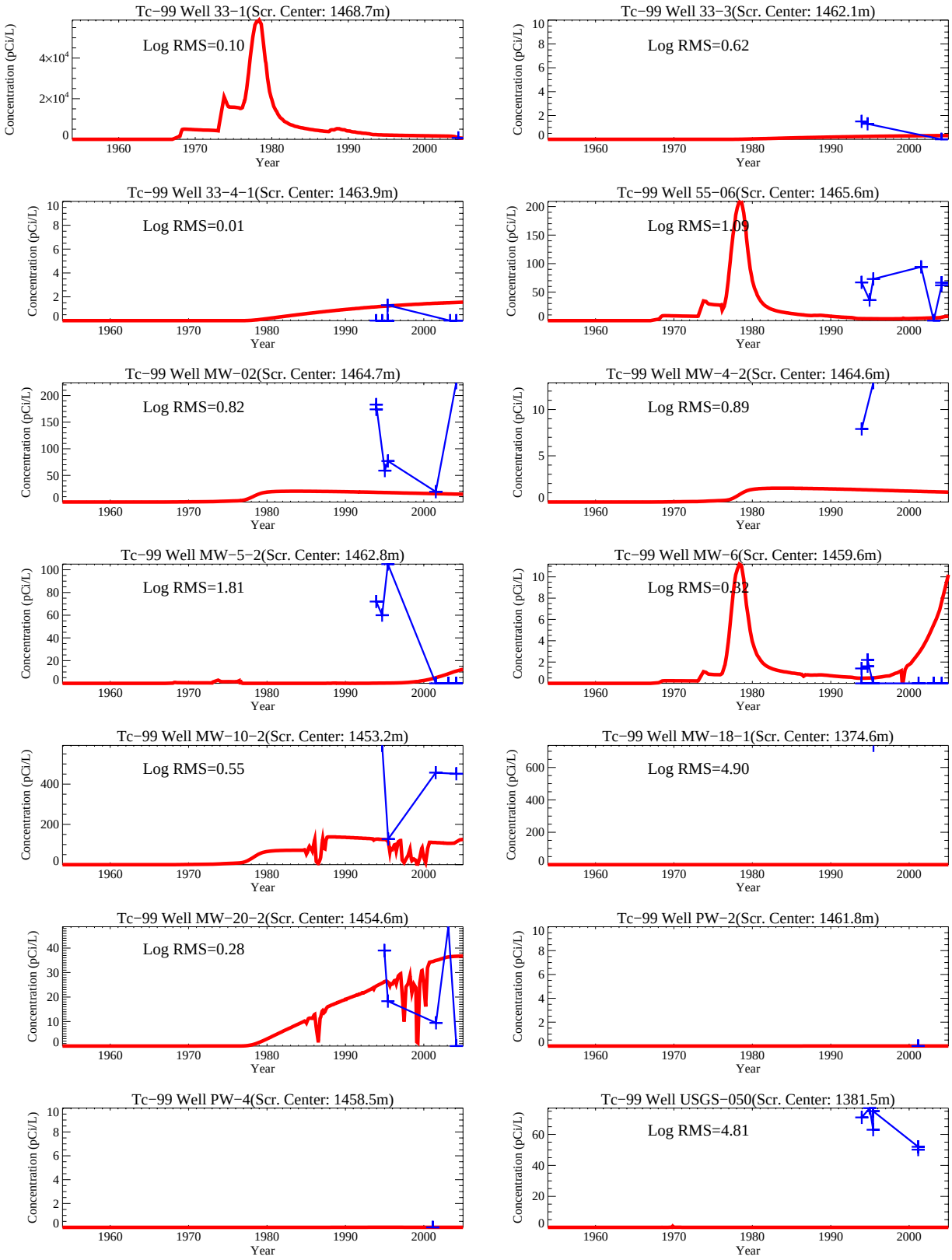

Figure A-10-21. Tc-99 concentration (pCi/L) in perched water wells for the 3-cm/year tank farm recharge rate case (measured values = blue crosses, red = model at screen center).

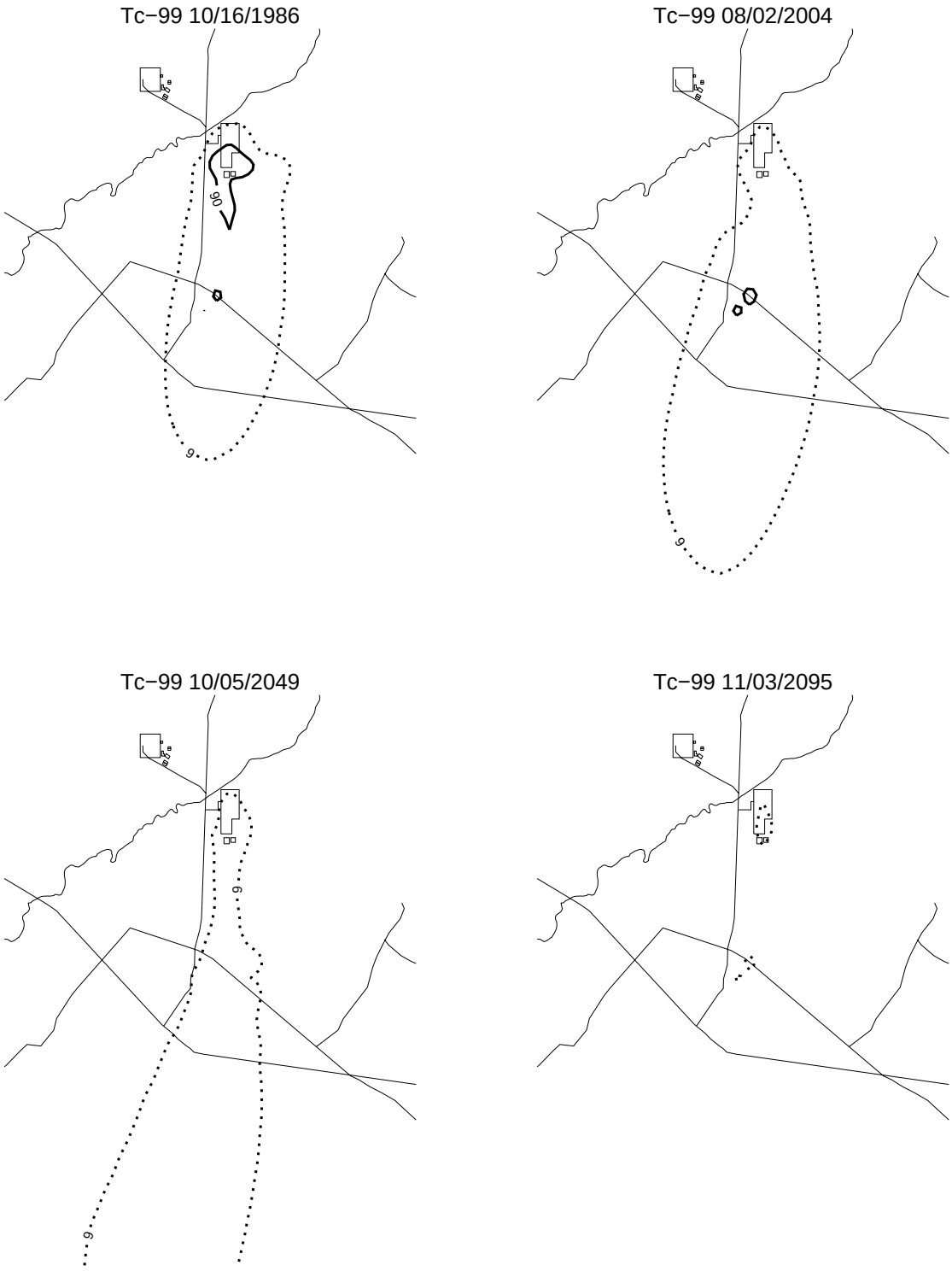

Figure A-10-22. Tc-99 aquifer concentrations (pCi/L) for the 3-cm/year tank farm recharge rate case (MCL*10 = thin red, MCL = thick red, MCL/10 = thin black, MCL/100 = thin black dashed).

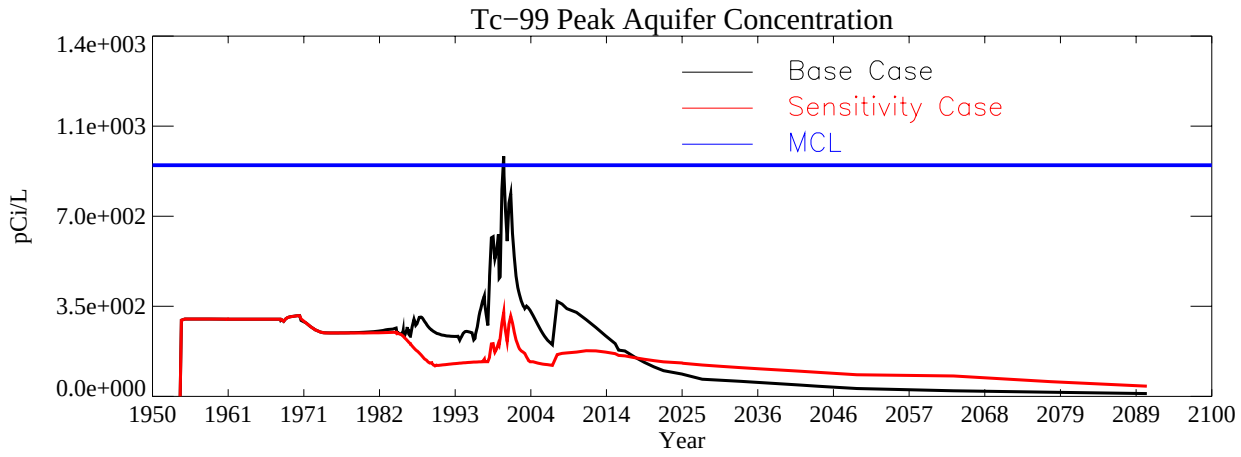

Figure A-10-23. Tc-99 peak aquifer concentration (pCi/L) for the 3-cm/year tank farm recharge rate case.

A-10.1.2.2 Tc-99 with 39-cm/year Tank Farm Recharge Rate

The peak simulated concentration in the vadose zone for this case was 1.49e+5 pCi/L in 1978 and is after the CPP-31 release date. The peak simulated concentration declined to 7.60e+3 pCi/L in 2005 and to 1.69e+3 pCi/L in 2095. Figures A-10-24 and A-10-25 illustrate the vertical and lateral extent of the simulated vadose zone concentrations. The shallow vadose zone contamination located immediately northwest of the former percolation ponds is due to the CPP-22 OU 3-13 soil site (0.1 Ci), which was placed in the model in 1990.

Figure A-10-26 illustrates the peak vadose zone concentration through time. The Tc-99 activity flux into the aquifer is illustrated in Figure A-10-27 and indicates that the tank farm Tc-99 is arriving slightly earlier than the base case. The Tc-99 concentration in key perched water wells is illustrated in Figure A-10-28.

The primary difference between the base case and the higher recharge sensitivity case is that the Tc-99 is transported through the vadose zone faster than the base case. This results in a slightly earlier breakthrough to the aquifer. However, breakthrough and aquifer concentrations were similar to the base case.

Figure A-10-29 illustrates the horizontal aquifer concentrations, and Figure A-10-30 illustrates peak aquifer concentrations through time. The peak aquifer concentration in the year 2095 was 10 pCi/L, which was similar to the base case.

Figure A-10-24. Tc-99 horizontal vadose zone concentrations (pCi/L) for the 39-cm/year tank farm recharge rate case (MCL = thick red, MCL/10 = thin black, MCL*10 = thin red).

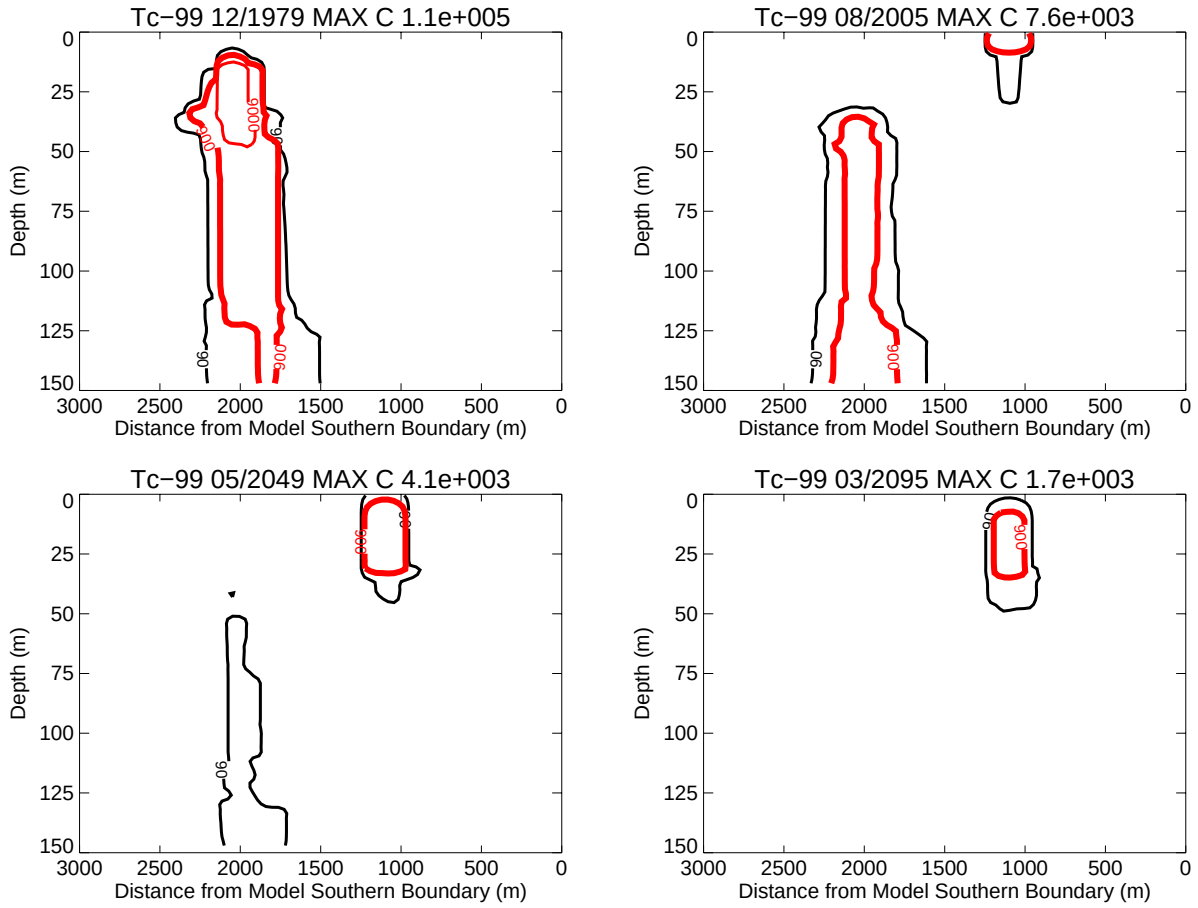

Figure A-10-25. Tc-99 vertical vadose zone concentrations (pCi/L) for the 39-cm/year tank farm recharge rate case (MCL = thick red, MCL/10 = thin black, MCL*10 = thin red).

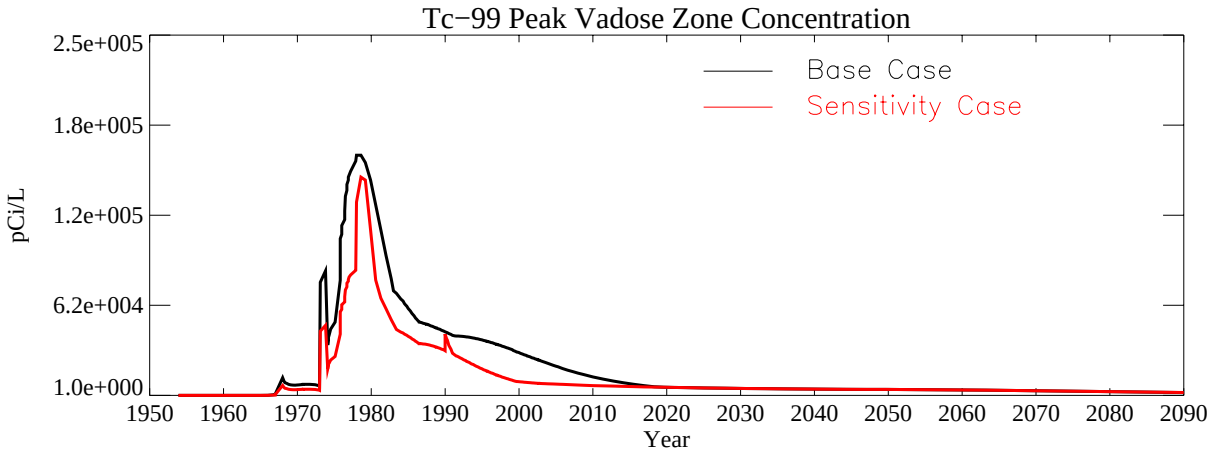

Figure A-10-26. Tc-99 peak vadose zone concentrations (excluding submodel area) (pCi/L) for the 39-cm/year tank farm recharge rate case.

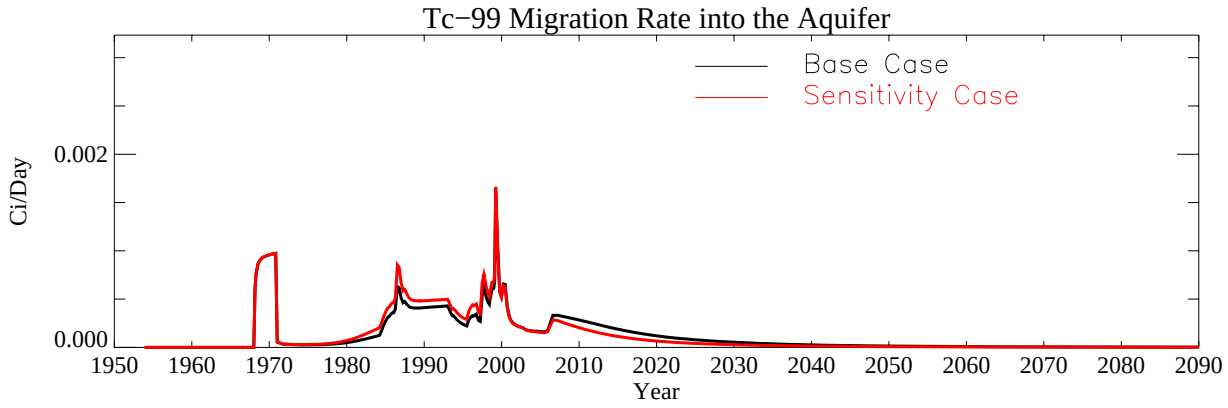

Figure A-10-27. Tc-99 flux into the aquifer (Ci/day) for the 39-cm/year tank farm recharge rate case.

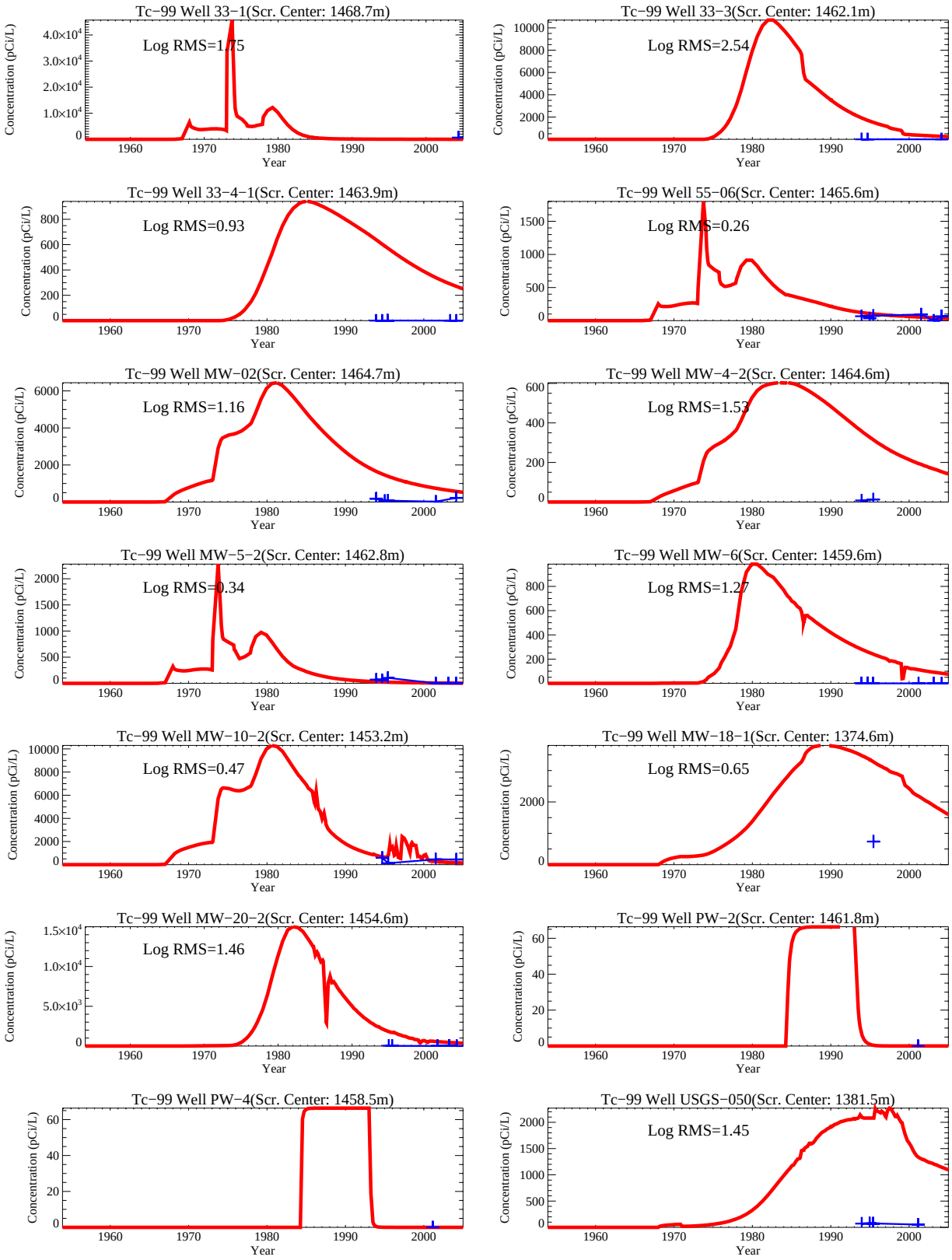

Figure A-10-28. Tc-99 concentration (pCi/L) in perched water wells for the 39-cm/year tank farm recharge rate case (measured values = blue crosses, red = model at screen center).

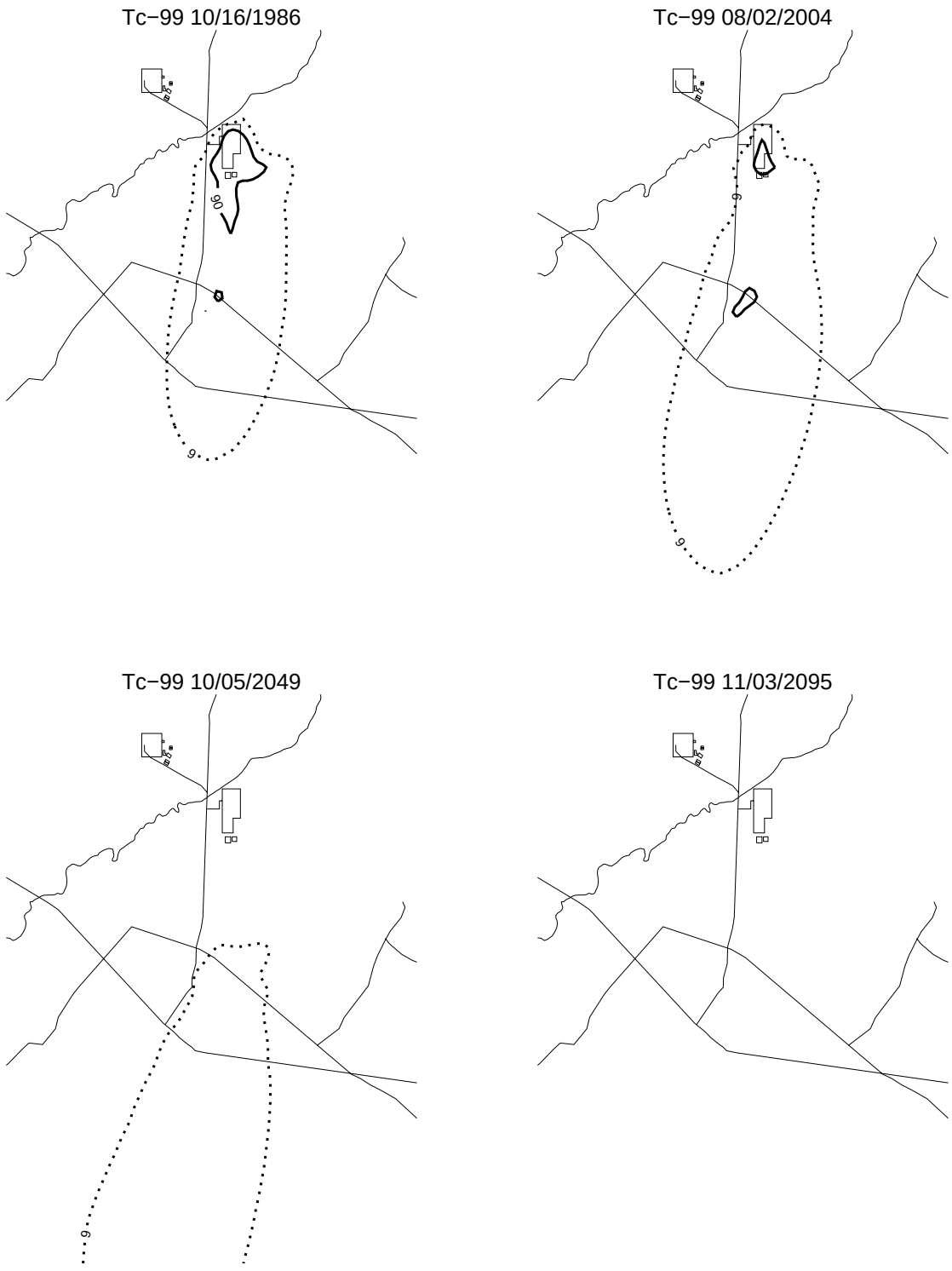

Figure A-10-29. Tc-99 aquifer concentrations (pCi/L) for the 39-cm/year tank farm recharge rate case (MCL*10 = thin red, MCL = thick red, MCL/10 = thin black, MCL/100 = thin black dashed).